

SUPPLEMENTAL MATERIAL

Cryo-Electron Microscopy Structure of the α IIb β 3–Abciximab Complex

Dragana Nešić,^{1,*} Yixiao Zhang,^{2,*} Aleksandar Spasic,^{3,*} Jihong Li,^{1,*} Davide Provasi,³ Marta Filizola,^{3,†} Thomas Walz,^{2,†} and Barry S. Collier^{1,†}

*D.N., Y.Z., A.S., and J.L. contributed equally to this work.

†M.F., T.W., and B.S.C. contributed equally to this work.

¹Allen and Frances Adler Laboratory of Blood and Vascular Biology, Rockefeller University, New York, NY; ²Laboratory of Molecular Electron Microscopy, Rockefeller University, New York, NY;

³Department of Pharmacological Sciences, Icahn School of Medicine at Mount Sinai, New York, NY

Short Title: Structure of the α IIb β 3-Abciximab Complex

Corresponding Author:

Barry S. Collier, M.D.

Allen and Frances Adler Laboratory of Blood and Vascular Biology

Rockefeller University

1230 York Avenue

New York, NY 10065

T: 212-327-7490

F: 212-327-7493

E: collerb@rockefeller.edu

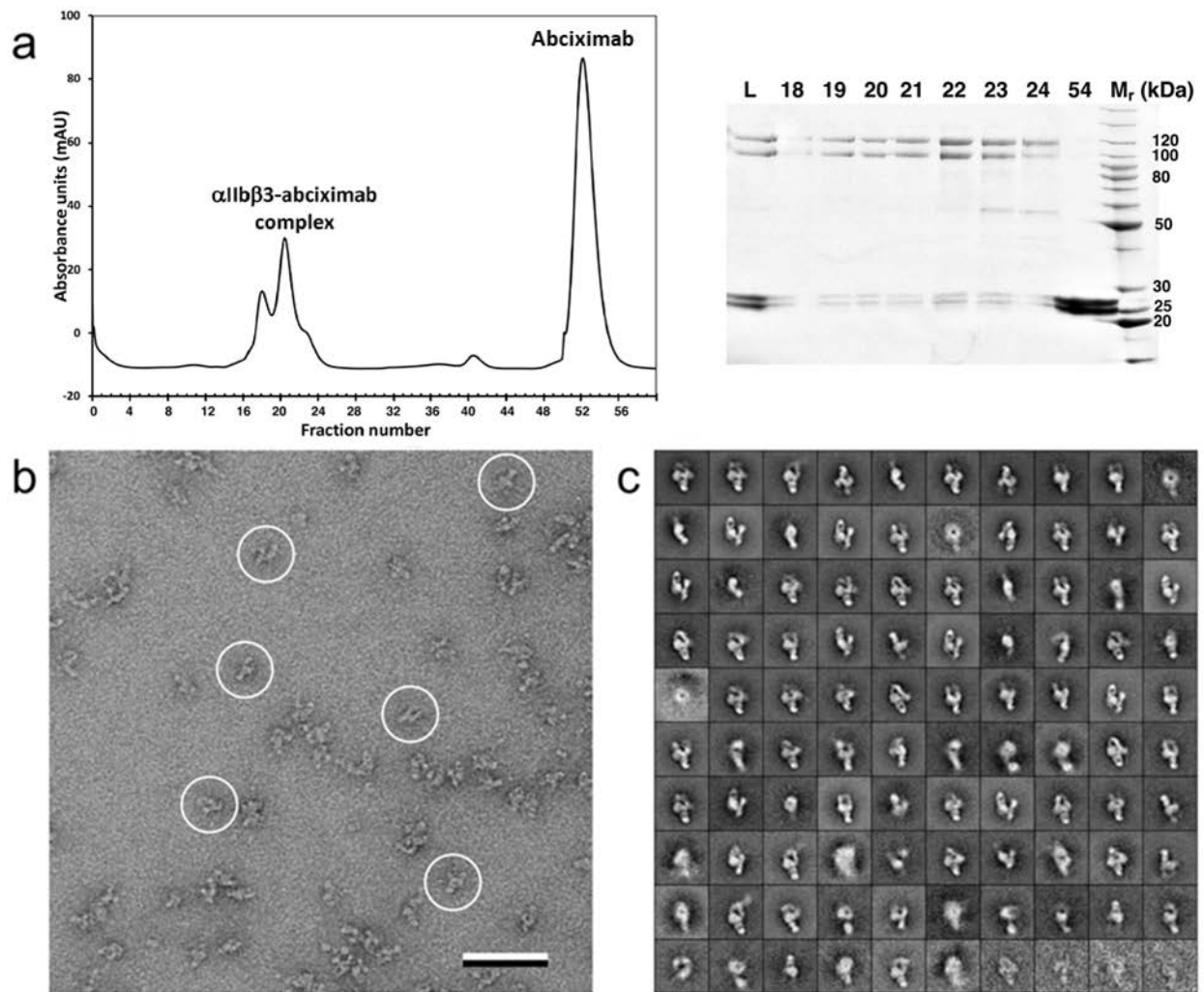
SUPPLEMENTAL TABLE I

Cryo-EM data collection, refinement and validation statistics

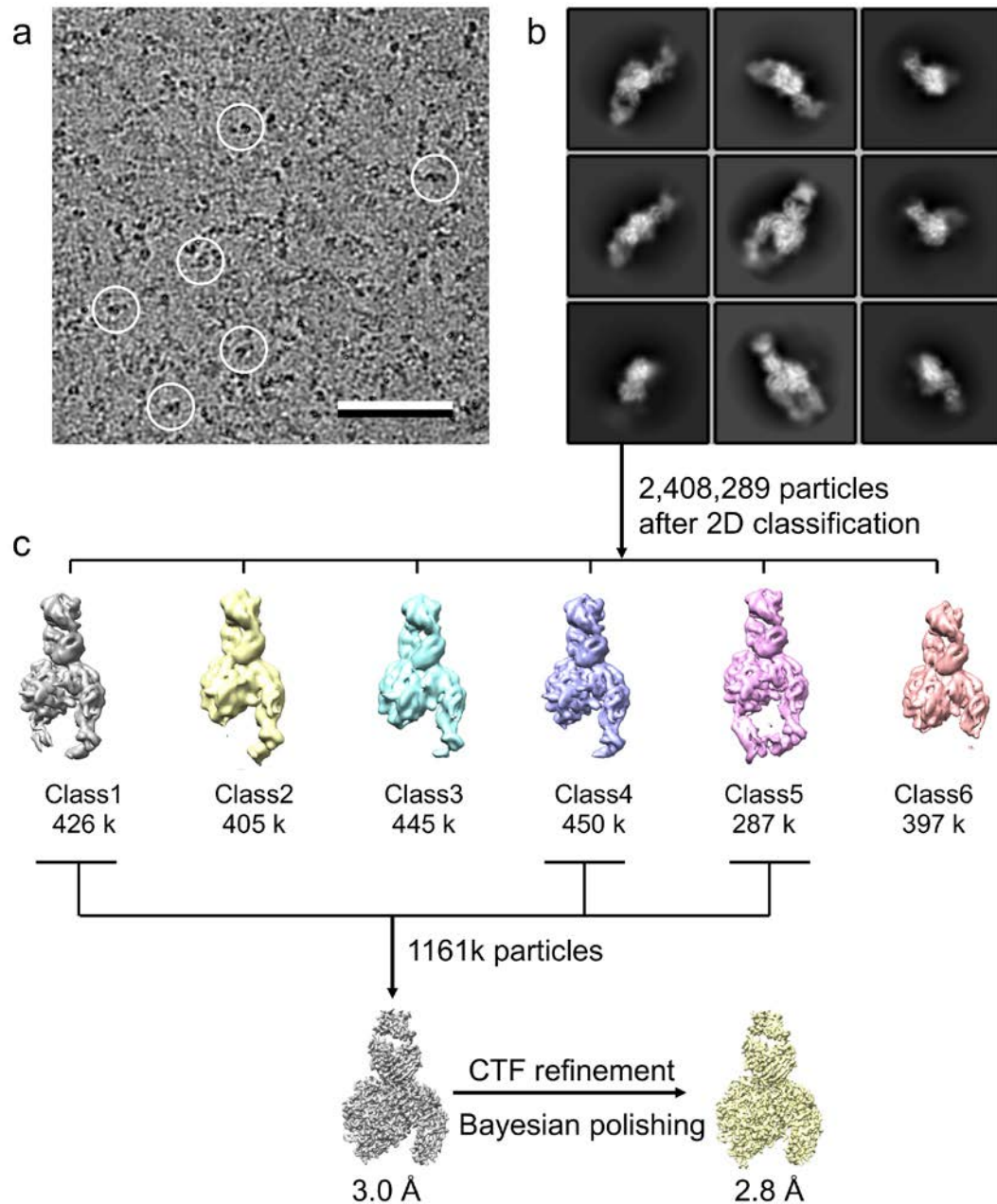
(Map: EMD-21044; Coordinates: PDB 6V4P)

Data collection and processing	
Magnification	28,000
Voltage (kV)	300
Electron exposure (e ⁻ /Å ²)	60
Defocus range (μm)	1.2~2.5
Pixel size (Å)	1.0
Symmetry imposed	C1
Image stacks (No.)	4,236
Initial particle images (No.)	2,970,080
Final particle images (No.)	1,161,396
Map resolution (Å)	2.8
FSC threshold	0.143
Map sharpening B factor (Å ²)	-105
Refinement	
R.m.s. deviations	
Bond lengths (Å)	0.004
Bond angles (°)	0.582
PDB validation	
Clash score	10.6
Rotamer outliers (%)	3.16
Cβ outliers	0
Overall score	2.22
Ramachandran plot	
Favored (%)	95.77
Allowed (%)	4.23
Outliers (%)	0

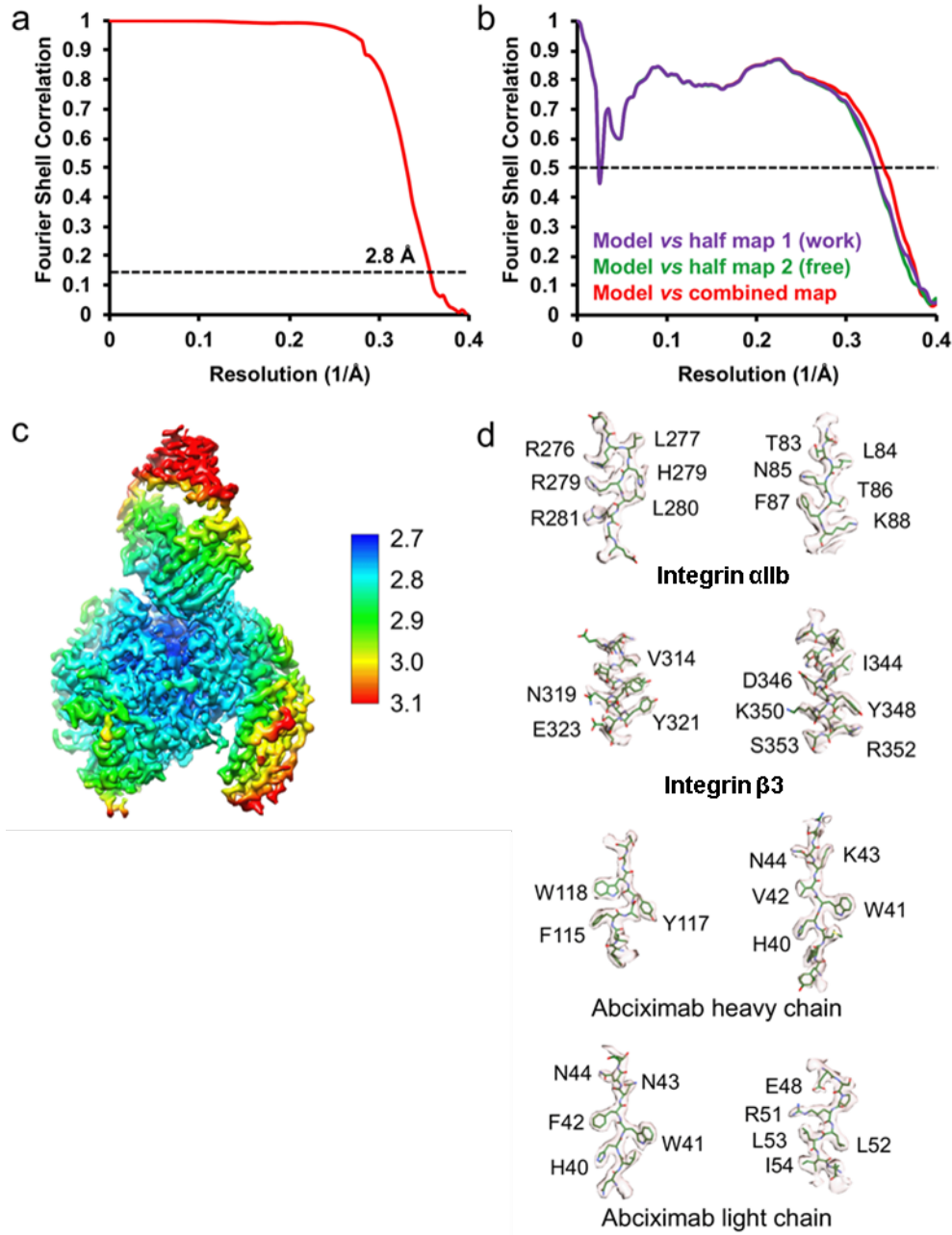
SUPPLEMENTAL FIGURES



Supplemental Figure I. Purification and negative-stain EM characterization of the $\alpha\text{IIb}\beta\text{3}$ -abciximab complex. (a) Left panel: Size-exclusion chromatography (Superdex™ Increase 200; 10/300 GL) profile of the purified integrin $\alpha\text{IIb}\beta\text{3}$ -abciximab complex. Right panel: Coomassie blue-stained 4-20% SDS-PAGE gel of different fractions from the size-exclusion chromatography column. L, loaded sample; Mr, molecular weight markers. (b) Area of an EM image of the negatively stained $\alpha\text{IIb}\beta\text{3}$ -abciximab complex. Some particles are circled. Scale bar: 25 nm. (c) The 100 2D-class averages of negatively stained $\alpha\text{IIb}\beta\text{3}$ -abciximab complex obtained by *K*-means classification of ~14,600 particles. The averages are shown from the most populous class at the top left to the least populous class at the bottom right. Side length of individual averages: 34 nm.



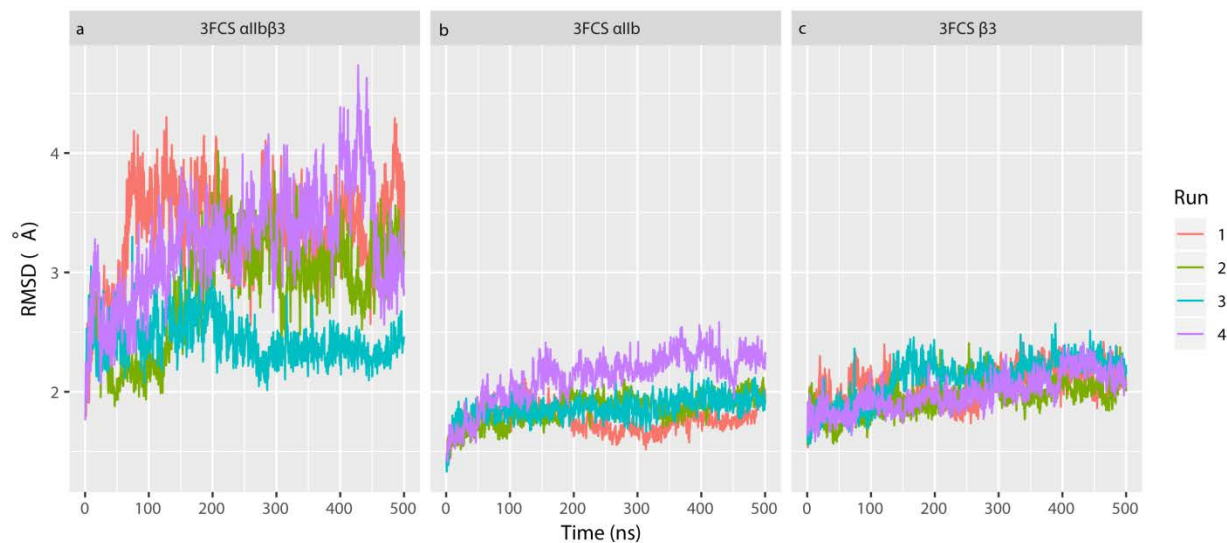
Supplemental Figure II. Cryo-EM image processing of the vitrified $\alpha\text{IIb}\beta\text{3}$ -abciximab complex. (a) Area of a cryo-EM image of the vitrified complex. Some particles are circled. Scale bar: 100 nm. (b) Selected 2D-class averages of vitrified $\alpha\text{IIb}\beta\text{3}$ -abciximab complex obtained with RELION-3. Side length of individual averages: 24 nm. (c) Image-processing workflow for 3D classification and refinement in RELION-3 that resulted in a density map of the $\alpha\text{IIb}\beta\text{3}$ -abciximab complex at 2.8 Å resolution. See Methods for details.



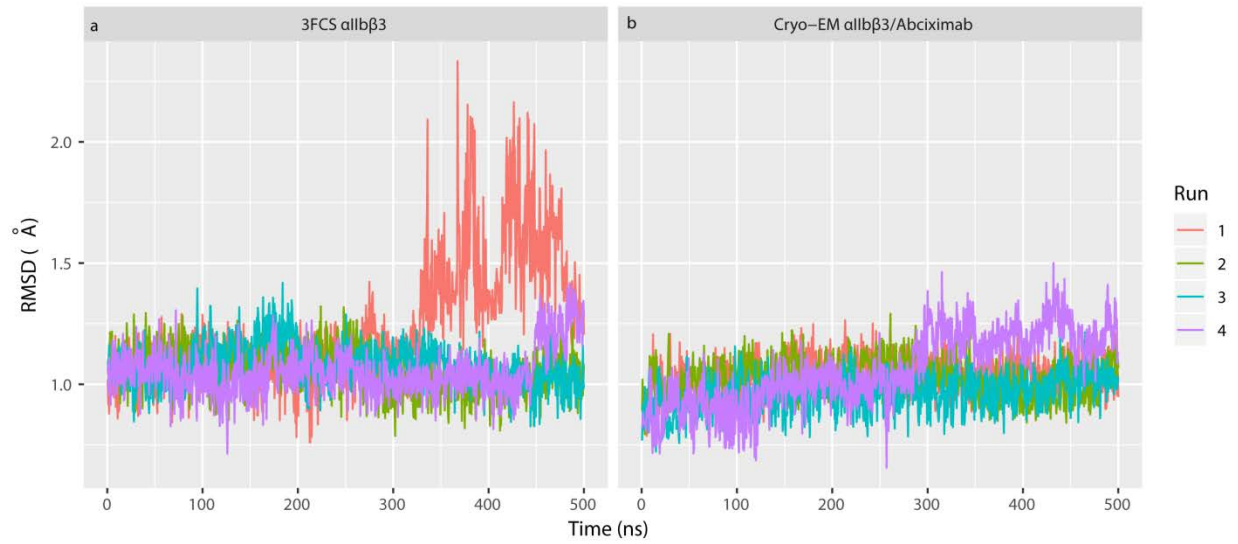
Supplemental Figure III. Characterization of the α IIb β 3–abciximab model. (a) Gold-standard FSC curve calculated between independently refined half maps for the density map of the α IIb β 3–abciximab complex. (b) Cross-validation FSC curves for the α IIb β 3–abciximab complex: purple, refined model *versus* half map 1, which was used for refinement (work map); green, refined model *versus* half map 2, which was not used for refinement (free map); red, refined model *versus* the combined final map. The similarity of the “work” and “free” curves suggests no substantial overfitting. (c) Local-resolution map of the α IIb β 3–abciximab complex. (d) Representative cryo-EM densities for the four polypeptide chains.



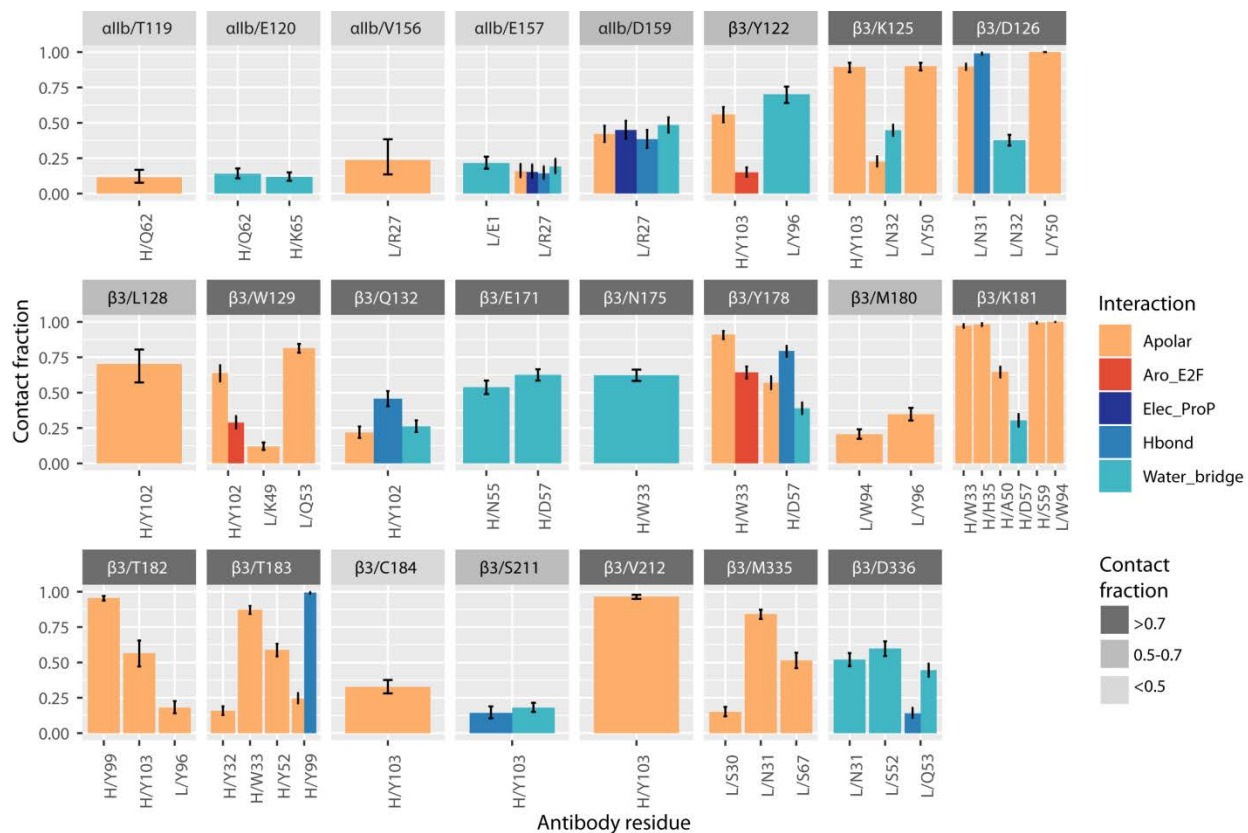
Supplemental Figure IV. All-atom mass-weighted RMSDs of the $\alpha\text{IIb}\beta\text{3}$ –abciximab complex from the starting cryo-EM structure. Different colors indicate different individual simulation runs. The RMSD over time is shown for: (a) the entire $\alpha\text{IIb}\beta\text{3}$ –abciximab complex, (b) the αIIb integrin subunit, (c) the β3 integrin subunit, (d) the abciximab heavy chain, (e) the abciximab light chain, (f) the variable region of the abciximab heavy chain, (g) the variable region of the abciximab light chain, (h) the constant region of the abciximab heavy chain, and (i) the constant region of the abciximab light chain.

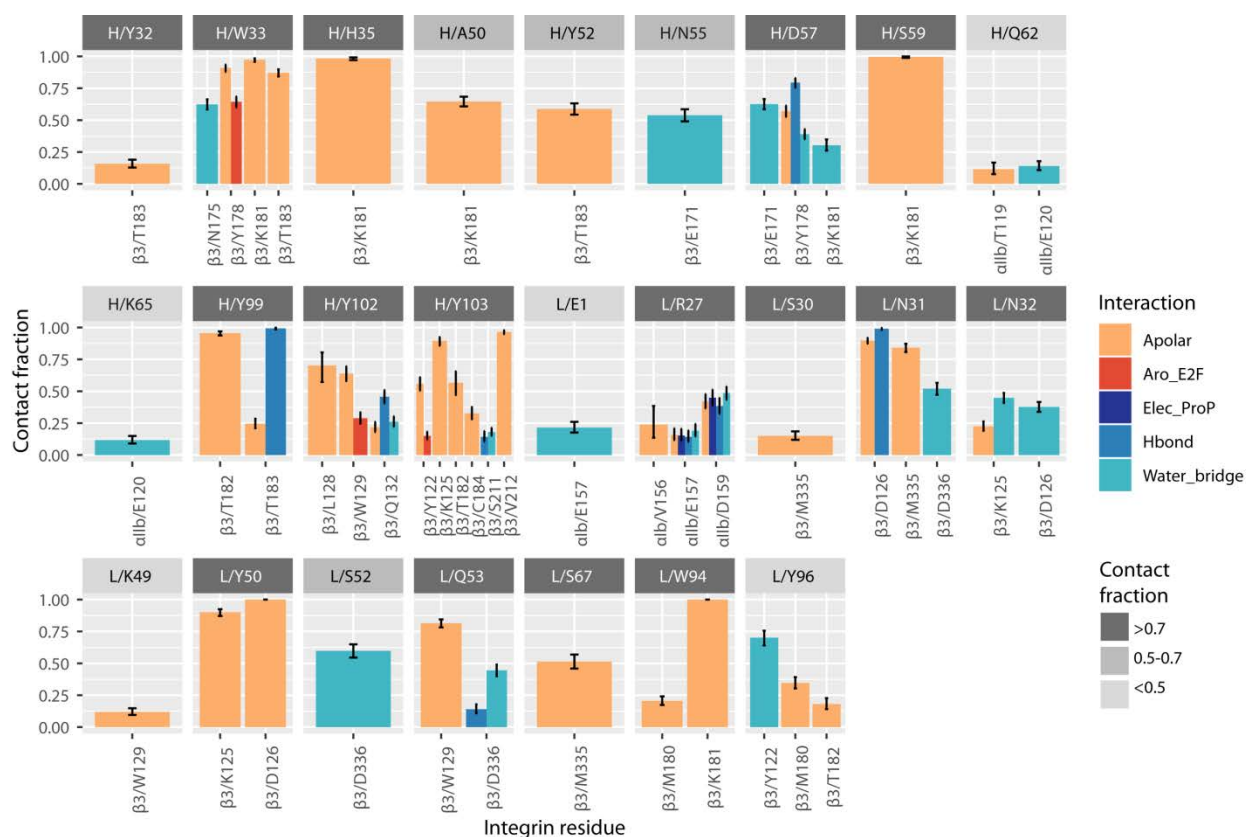


Supplemental Figure V. All-atom mass-weighted RMSDs of allb β 3 integrin from the starting X-ray crystal structure (PDB: 3FCS).¹ Different colors indicate different individual simulation runs. The RMSDs over time are shown for (a) the entire allb β 3 integrin, (b) the allb integrin subunit, and (c) the β 3 integrin subunit.

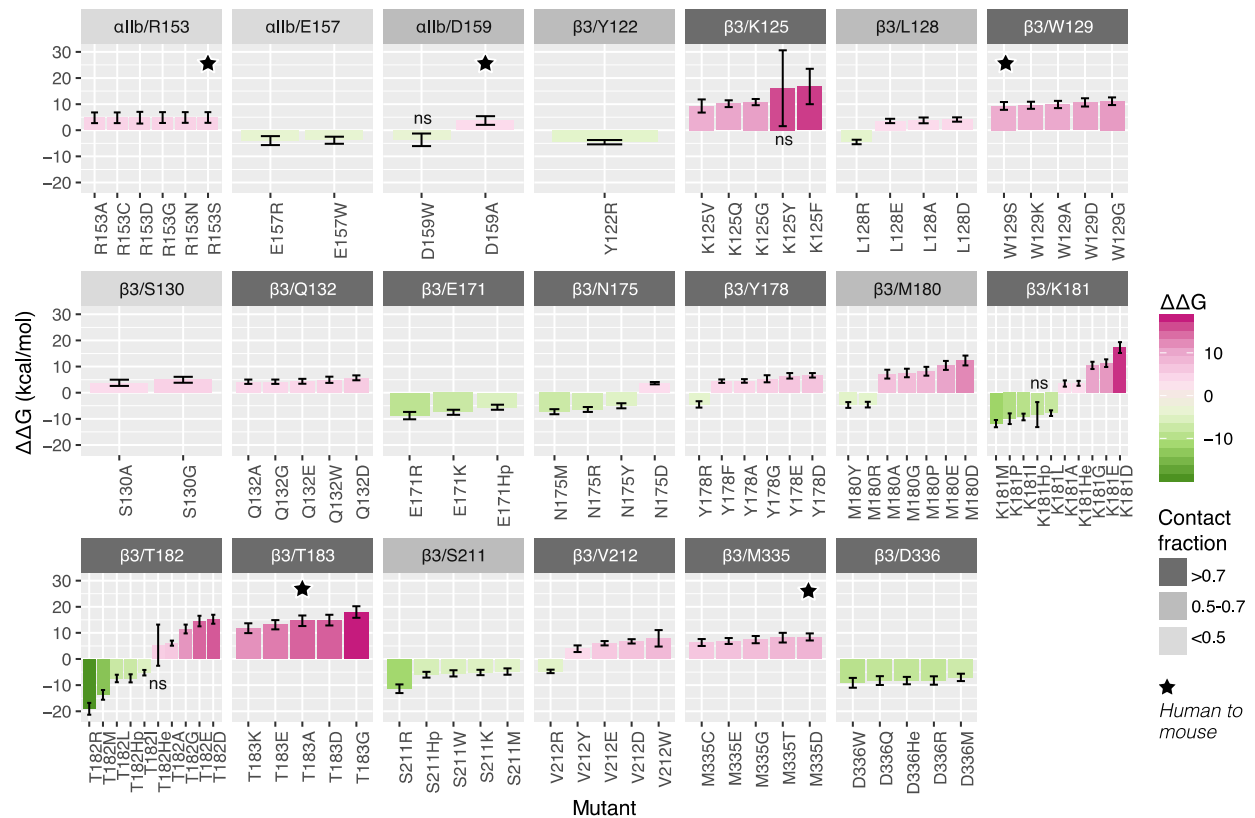


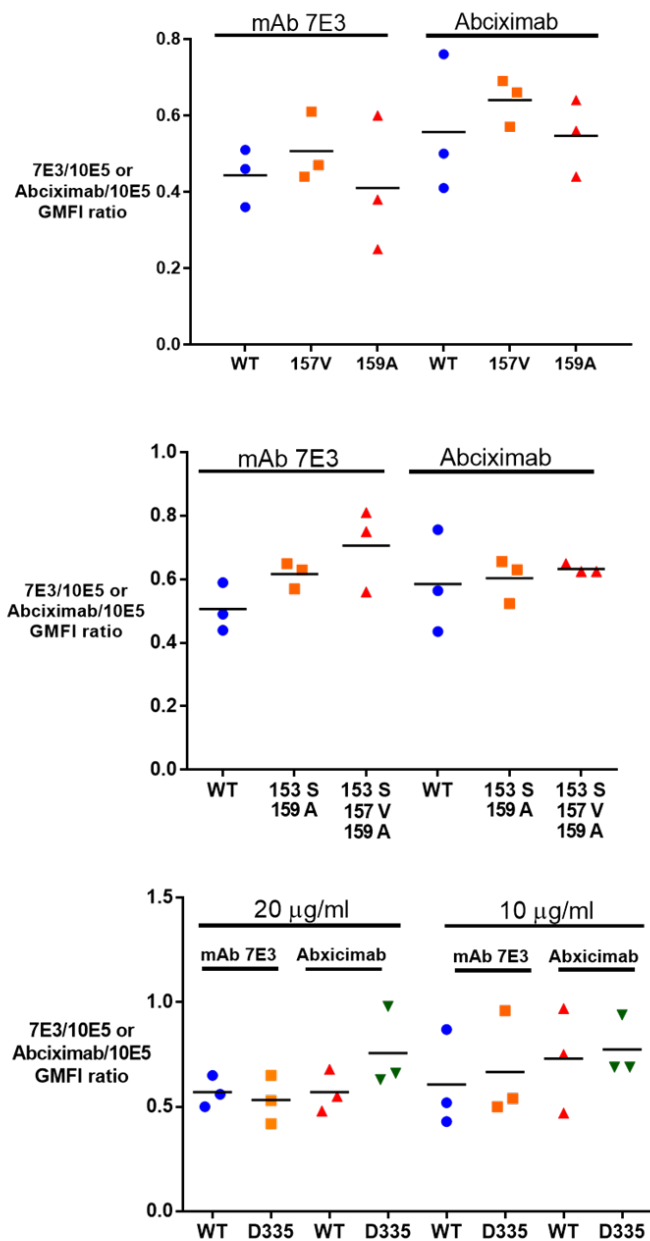
Supplemental Figure VI. All-atom mass-weighted RMSDs of the fibrinogen/RGD-binding pocket from the starting X-ray crystal structure and cryo-EM model, respectively. The RMSD over time is shown for (a) the fibrinogen/RGD-binding pocket in the structure of the unliganded $\alpha\text{IIb}\beta\text{3}$ integrin with respect to the starting X-ray crystal structure (PDB: 3FCS)¹ and (b) the fibrinogen/RGD-binding pocket in the structure of the $\alpha\text{IIb}\beta\text{3}$ –abciximab complex with respect to the starting cryo-EM structure. Different colors indicate results from individual simulation runs.



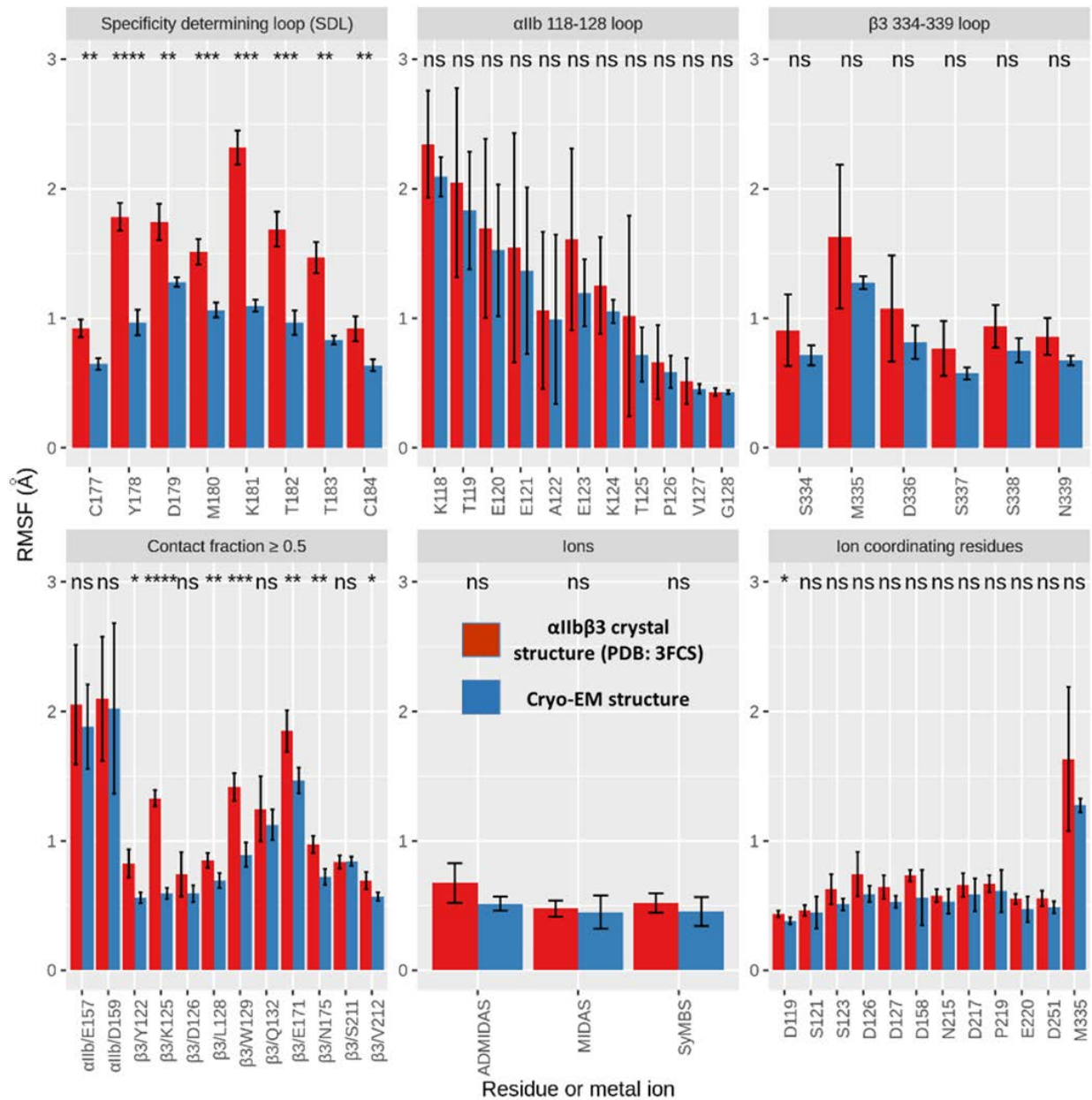


Supplemental Figure VIII. Interaction fingerprints of abciximab residues within a 4.5-Å distance from $\alpha\text{IIb}\beta\text{3}$ integrin residues in at least 10% of simulation frames. Only side-chain atoms were considered for these calculations. Different types of interaction are represented by different color bars (orange: non-polar interactions; red: aromatic edge-to-face interactions; dark blue: electrostatic interactions; light blue: hydrogen bonds; cyan: water-mediated hydrogen bonds). The grey hue used for the background of residue labels denotes the percentage of frames a given residue is engaged in an intermolecular interaction (contact fraction) (dark grey: contact fraction of at least 0.7; intermediate grey: contact fraction between 0.5 and 0.7; light grey: contact fraction below 0.5).





Supplemental Figure X. Binding of mAb 7E3 and abciximab to cells expressing normal $\alpha IIb\beta 3$ and $\alpha IIb\beta 3$ containing mutations of residues that make contact with abciximab. Cells were analyzed for the binding of fluorescently-labeled $\alpha IIb\beta 3$ mAb 10E5 to assess total $\alpha IIb\beta 3$ expression and separately for the binding of fluorescently-labeled mAb 7E3 or abciximab by flow cytometry. The geometric mean fluorescence intensity (GMFI) of cells treated with mAb 7E3 or abciximab was determined and is presented as a fraction of the GMFI of cells treated with mAb 10E5. The normal (WT) $\alpha IIb\beta 3$ residues are αIIb Arg153, Glu157, and Asp159, and $\beta 3$ Met335. All experiments were conducted three times and all of the data points are reported.



Supplemental Figure XI. Assessment of the dynamics of individual residues and β3 metal ions by Root Mean Square Fluctuation (RMSF) analysis in the absence and presence of abciximab. The RMSF values from four separate 500-ns MD simulations of the cryo-EM structure of the $\alpha\text{IIb}\beta\text{3}$ -abciximab complex for each indicated residue were combined and are expressed as the mean \pm SD (blue bars). For comparison, the same analysis was performed on the crystal structure of $\alpha\text{IIb}\beta\text{3}$ in the absence of abciximab (red bars). The categories of residues studied were: 1. the residues in the SDL; 2. the residues in the αIIb 118-128 loop; 3. the residues in the β3 334-339 loop; 4. the residues with contact fractions ≥ 0.5 ; 5. the β3 metal ions; 6. the residues coordinating the β3 metal ions. ns, not significant; *, $p \leq 0.05$; **, $p \leq 0.01$; ***, $p \leq 0.001$; ****, $p \leq 0.0001$

References

1. Zhu J, Luo BH, Xiao T, Zhang C, Nishida N and Springer TA. Structure of a complete integrin ectodomain in a physiologic resting state and activation and deactivation by applied forces. *Mol Cell*. 2008;32:849-861.

Major Resources Tables

Antibodies

Target antigen	Vendor or Source	Catalog #	Working concentration	t # (preferred but not required)	Persistent ID / URL
10E5	NCCC	MH1386	10-20 µg/ml		
7E3	NCCC	94PR0032	10-20 µg/ml		
abciximab	Centocor/Lilly	05A05AA	10-20 µg/ml		
AP5	Dr. Peter Newman	N/A	10-20 µg/ml		

DNA/cDNA Clones

Clone Name	Sequence	Source / Repository	Persistent ID / URL
Integrin α11b/pEF1/V5-His A	Artoni et al. PMID 15277669,2004	Junichi Takagi, Harvard University, Boston	
Integrin β3/pcDNA3.1/myc-His A	Wang et al. PMID 9351872,1997	Dr. Peter Newman	

Cultured Cells

Name	Vendor or Source	Sex (F, M, or unknown)	Persistent ID / URL
HEK 293	ATCC	F	CRL 1573

Data & Code Availability

Description	Source / Repository	Persistent ID / URL
Cryo-EM density map	EMDB	21044
Model atomic coordinates and abciximab amino acid sequence	PDB	6V4P
Molecular dynamics (MD) data (initial coordinates and topologies, as well as simulation trajectories)	Open Science Framework	https://osf.io/jqcxk/ DOI 10.17605/OSF.IO/JQCXK
Modeling missing loops, MM-GBSA mutation estimates	Schrödinger	https://www.schrodinger.com/
Package for MD simulations	Gromacs	http://www.gromacs.org/
Software for MD data analysis	Cpptraj and in-house Python script	http://ambermd.org and https://www.python.org/
Software for figure illustration of MD data	In-house R script and tidyverse	https://www.r-project.org/ and https://www.tidyverse.org/
Software for making figures of 3D structures from MD data	Chimera	https://www.cgl.ucsf.edu/chimera/